RSC Advances

Accepted Manuscript

This article can be cited before page numbers have been issued, to do this please use: R. Arumugaperumal, V. Srinivasadesikan, M. C. Lin, M. Shellaiah, T. Shukla and H. Lin, *RSC Adv.*, 2016, DOI: 10.1039/C6RA24472F.

ROYAL SOCIETY OF CHEMISTRY

rsc.li/rsc-advances

View Article Online
DOI: 10.1039/C6RA24472F

Journal Name

ARTICLE

Facile rhodamine-based colorimetric sensors for sequential detections of Cu (II) ion and pyrophosphate ($P_2O_7^{4-}$) anion

Received 00th January 20xx,
Accepted 00th January 20xx

DOI: 10.1039/x0xx00000x

www.rsc.org/

Reguram Arumugaperumal,[a] Venkatesan Srinivasadesikan,[b] Ming-Chang Lin,[b] Muthaiah Shellaiah,[a] Tarun Shukla[a] and Hong-Cheu Lin[a]*

Abstract:

Two rhodamine hydrazine derivatives **Rh1** and **Rh2** with catechol and ether functionalities have been synthesized and utilized towards sequential colorimetric detections of Cu(II) and pyrophosphate (PPi) ions in CH_3CN–H_2O (v/v = 9:1, 5mM Tris-HCl, pH 7.4) semi-aqueous medium. Notably, **Rh1** and **Rh2** are the first example of colorimetric rhodamine-based probes for the sequential detections of Cu^{2+} ion and PPi anion. Based on the significant colorimetric responses (from colorless to pink) of **Rh1** and **Rh2** to Cu^{2+} ions, the detection limits were estimated as low as $1.22x10^{-8}$ M and $8.0x10^{-7}$ M, respectively, which signified the utilities of designed probes towards facile detections of Cu^{2+} ions. Furthermore, upon the successive addition of PPi ion to **Rh1**-Cu^{2+} and **Rh2**-Cu^{2+} complexes, it has been altered and restored to its origin of **Rh1** and **Rh2** *via* re-coordination of PPi to Cu^{2+} ion, which was confirmed by color changes from pink to colorless. Moreover, computational DFT calculations provided more insights into HOMO-LUMO structures of rhodamine derivatives and their copper complexes. Additionally, the solid state strip-based colorimetric detections of Cu^{2+} ion were supplemented as a real time application.

Introduction

Recently, owing to the environmental and biological significance, new artificial materials have been emerged as efficient chemosensors towards the detections and estimation of transition metal ions.[1-3] Among them, copper ions were found to be essential and its detection has been paid greater attention over other metal ions.[4-7] In this concern, divalent copper ion is more fascinating because not only as an environmental pollutant at higher concentrations but also as the third most abundant divalent metal ion in the human body. [8-12]

Furthermore, copper has been suspected to cause liver and kidney damages for infants in long-term exposure. Similarly, short-term exposures to high levels of copper ion cause gastrointestinal disturbance.[13-14] Henceforth, the U.S. Environmental Protection Agency (EPA) has set a limit of copper ions in drinking water as 1.3 ppm (ca. 20 mM).[15] Additionally, the average concentration of blood copper in the normal body is fixed as 100–150 mg dL^{-1} (15.7-23.6 mM).[16] However, copper can be toxic over its normal concentration that cause oxidative stresses and disorders associated with neurodegenerative diseases, including Meknes, Wilson diseases, familial amyotrophic lateral sclerosis, Alzheimer's disease and prion diseases. Therefore, the colorimetric visual detection of trace amounts of Cu^{2+} ions *via* simplified instrumental set up are become vital.[17-21] In this concept, the high sensitivity and selectivity are considered as a fundamental goal for organic and analytical chemists all over the world. In order to achieve the selective detection of Cu^{2+} against the background of competing analytes, many promising small molecules have been reported as Cu^{2+} sensor through colorimetric response.[22]

On the other hand, Phosphate-based inorganic and organic molecules play critical roles in both environment and biological systems. Among phosphate anions, pyrophosphate (PPi) is known to be biologically significant one [23], which has been obtained as a product, during the hydrolysis of adenosine triphosphate (ATP) to adenosine monophosphate under cellular condition.[24] However, abnormal levels of PPi can lead to several diseases such as chondrocalcinosis or calcium pyrophosphate dihydrate (CPPD) crystal deposition problem and arthritis.[25] Recently, several approaches such as electro optical methods, colorimetric and fluorescence assays have been developed for the detection of PPi ions.[26-28] Among those techniques, colorimetric chemosensors are most attractive for the detection of PPi due to their selectivity, sensitivity, response time

[a] Department of Materials Science and Engineering, National Chiao Tung University, Hsinchu 300, Taiwan
[b]Center for Interdisciplinary Molecular Science, Department of Applied Chemistry, National Chiao Tung University, Hsinchu 300, Taiwan.
† Electronic supplementary information (ESI) available: NMR and mass spectra of **Rh1** and **Rh2** and sensor properties mentioned in the text.See DOI: 10.1039/b000000x/

View Article Online
DOI: 10.1039/C6RA24472F

and low-cost. [29] Moreover, because of the strong binding affinities between metal ions and PPi, the utilization of metal ion complexes as a colorimetric chemosensor has been found to be the successful strategy for the detection of PPi ions. However, chemosensors based on color changes (by naked eye observation) for detection of PPi are found to be limited.[30] Hence, we tend to develop such colorimetric sensors for the detection of PPi ions.

On the consideration of photophysical properties, such as high quantum yield, photo stability, absorption and emission in the visible region, rhodamine fluorophore is seems to be most attractive one.[31-34] Further, the sensing behavior of rhodamine towards metal ions is also very interesting. Typically, rhodamine derivatives are non-fluorescent and colorless in their ring-closed spiro lactam structures, whereas the spiro lactams induced ring-opening by specific metal-give rise to strong fluorescence emissions to develop for colorimetric sensors.[35-38] Nevertheless, many rhodamine–based florescent and colorimetric chemosensors for detecting metal ions have been studied.[39] Colorimetric sensors are more facile due to the detection by naked eye that can be commonly used in low cost, less equipment and easy handling.[40-45] There are perceptible color changes in Rhodamine derivatives, even at very small amounts of analyte concentrations. Therefore, much effort has been focused on the development of rhodamine-based sensor probes for the detections of heavy metal and anions[46]. On the other hand, direct detections of Cu(II) and PPi ions could be accomplished by regulating the acceptors of rhodamine sensor molecules to affect ICT mechanisms, which may evidence via ratiometric responses and ion induce naked-eye color changes[47]. Hence, rhodamine-based chemosensory probes for the sequential recognitions of Cu(II) and PPi ions remained highly demands. Yoon and co-workers previously demonstrated rhodamine derivative as a chemosensor for sequential detections of Al^{3+} and pyrophosphate.[48] However, to the best of our knowledge, rhodamine-based selective and sensitive sequential detections of Cu^{2+} and pyrophosphate *via* the ratiometric absorption spectral changes have never been explored yet.

Herein, we have successfully developed two reversible colorimetric chemosensor probes **Rh1** and **Rh2** for sequential detections of Cu^{2+} and pyrophosphate (PPi) ions. Dimers **Rh1** and **Rh2** (Fig.1) contain two symmetrical rhodamine units (on both ends) as the fluorophore and two central cores of dihydroxyphenyl and multiple ethers groups as the chelating units, respectively. The receptor moieties together with the nitrogen and carbonyl of rhodamine serve as ionophores by providing coordinating sites based on spirocyclic ring-opening mechanisms. Additionally, the optical properties of these probes and their possible mechanisms for recognition of Cu^{2+} ion has been demonstrated by UV-Vis titrations. Further, B3LYP/LANL2DZ density functional calculations were carried out to investigate the molecular orbitals and electronic excitations of these two probes. The stabilities of two probes were examined in the absence and presence of Cu^{2+} ion at wide ranges of pH values. Interestingly, both metal complexes (**Rh1**-Cu^{2+} and **Rh2**-Cu^{2+}) have been utilized in excellent selective detections of PPi via colorimetric changes visualized by naked-eyes.

2. Experimental

2.1 Materials and instrumentations

All reagents were commercially purchased and were used without further purification. The solvents were dried by distillation over appropriate drying agents. Generally, reactions were monitored by TLC plates and flash chromatography was performed on silica gel. The ^1H and ^{13}C NMR spectra were recorded on a 300 MHz spectrometer and samples were dissolved in $CDCl_3$ and DMSO-*d6*. The chemical shifts were expressed in ppm and coupling constants (J) in Hz. Mass spectra (FAB) were obtained on the respective mass spectrometer. Elemental analysis was carried out by Elemental Varo EL. UV-vis absorption and fluorescence spectra were measured on V-670 spectrophotometer and F-4500 fluorescence spectrophotometer, respectively. The pH [1-12] buffer solutions were freshly prepared.

2.2 Preparation of metal ion solutions for sensor titrations

Rh1 and **Rh2** were dissolved in in CH_3CN–H_2O (v/v = 9:1, 5mM Tris-HCl, pH 7.4) at 1 x 10^{-5} M concentration. The solutions of metal cations Li^+, K^+, Cs^+, Ni^{2+}, Fe^{3+}, Fe^{2+}, Co^{2+}, Zn^{2+}, Cd^{2+}, Pb^{2+}, Ca^{2+}, Cr^{3+}, Cu^{2+}, Ba^{2+} and Al^{3+} were dissolved in water medium at 1x10^{-3} M concentration from their chloride salts. Ag^+, Hg^{2+} and Mg^{2+} were made from $AgNO_3$, Hg $(OAc)_2$ and $MgSO_4$, respectively, in water medium at 1x10^{-3} M concentration. The solutions of all anions were prepared by dissolving the respective TBA salts of F^-, CN^-, HPO_4^{2-}, $H_2PO_4^-$, HSO_4^-, ClO_4^-, Br^-, OH^-, SCN^-, $P_2O_7^{4-}$, NO_3^- and OAc^- in deionized water (1 X 10^{-3} M). Pentamethyl diethylene triamine (PMDTA) was dissolved in CH_3CN at a concentration of 1x10^{-3} M.

2.3 NMR titrations

10 mmol (1 equiv.) of **Rh1** and **Rh2** in DMSO-d6 were titrated with 20 mmol (2 equiv.) of Cu^{2+} in D_2O.

2.4 Computational methods

Density functional theory (DFT) calculations were employed to elucidate the Cu^{2+} interactions with **Rh1** and **Rh2** systems. All computations were carried out using Gaussian 09 software package[49]. Geometry optimization of the ground state structures was carried out with DFT at the B3LYP level of theory using LANL2DZ basis set in gas phase [50]. The excitation energies (up to 5 states) of the low-lying excited states and oscillator strengths were predicted using the time-dependent density functional theory (TD-DFT) with B3LYP/LANL2DZ level.

2.5 Synthetic procedures

The following compounds (1-3) were prepared according to the literature: 2,3-dihydroxyterephthalaldehyde (1),[51] [2,2'-(oxybis (ethane-2,1 diyl)bis(oxy)dibenzaldehyde (2)[52] and rhodamine hydrazide [53]. The detailed synthetic procedures are illustrated in the supporting information and Scheme S1.

2.5 Synthesis of compound Rh1

Rhodamine hydrazide 3 (0.6 g, 1.32 mmol) was dissolved in absolute ethanol (25 mL), then 3,6-diformylcatechol (1) (0.1 g, 0.66 mmol) was added and the reaction mixture was refluxed in an oil bath for 12 h. The solvent was evaporated by rotary evaporator and the crude product was purified by silica gel column chromatography

View Article Online
DOI: 10.1039/C6RA24472F

using EA:hexane (1:1, v/v) to obtain compound **Rh1** as a light pink solid. Yield: 0.32 g (50%). ^{1}H NMR ($CDCl_3$) δ: 10.62 (s, 2H), 9.16 (s, 2H), 7.95-7.93 (m, 2H), 7.51-7.45 (m, 4H), 7.12-7.10 (m, 2H), 6.57 (s, 2H), 6.47 (d , 4H, J = 3.0 Hz), 6.41 (d, 4H, J = 2.7 Hz), 6.21 (dd, 4H, J = 8.7 Hz and 2.4 Hz), 3.30 (q, 16H, J = 6.9 Hz), 1.12 (t, 24H, J = 6.9 Hz); ^{13}C NMR ($CDCl_3$) δ: 164.3, 153.2, 152.5, 151.5, 148.9, 146.9, 133.9, 129.2, 128.3, 127.8, 124.0, 123.2, 120.8, 119.5, 108.0, 105.0, 98.1, 66.4, 44.3, 12.5; IR (KBr, cm^{-1}): 3425, 3079, 1706; MS (FAB^+) m/z: calcd for $C_{64}H_{66}N_8O_6$: 1042.5; found: 1143.7 $(M+H)^+$; Anal. calcd. for $C_{64}H_{66}N_8O_6$: C, 73.68; H, 6.38; N, 10.74; found: C, 72.66; H, 6.60; N, 10.75.

2.6 Synthesis of compound Rh2

Rhodamine hydrazide 3 (0.5 g, 1.26 mmol) was dissolved in absolute ethanol (25 mL), then 2,2'-((oxybis(ethane-2,1-diyl)) bis(oxy))dibenzaldehyde (2) (0.2 g, 0.63 mmol) was added and the reaction mixture was refluxed in an oil bath for 12 h. The solvent was evaporated by rotary evaporator and the crude product was purified by silica gel column chromatography using EA:hexane (6:4, v/v) to obtained compound **Rh2** as a light pink solid. Yield: 0.310 g (40%). ^{1}H NMR ($CDCl_3$) δ: 9.03 (s, 2H), 7.97 (dd, 2H, J = 1.8 Hz and 5.4 Hz), 7.85-7.83 (m, 2H), 7.48- 7.44 (m, 4H), 7.17-7.09 (m, 4H), 6.84 (t, 2H, J = 7.5 Hz), 6.76 (d, 2H, J = 8.4 Hz) , 6.53 (d, 4H, J = 9.0 Hz), 6.43 (d, 4H, J = 2.4), 6.22 (dd, 4H, J = 8.7 Hz and 2.4 Hz), 4.01 (t, 4H, J = 5.1 Hz) ,3.82 (t, 4H, J = 5.1 Hz), 3.28 (q, 16H, J = 6.9 Hz), 1.11 (t, 24H, J = 6.9 Hz); ^{13}C NMR ($CDCl_3$) δ: 164.9, 157.3, 153.6, 153.1, 149.8, 143.6, 133.1, 130.8, 129.3, 128.1, 127.4, 126.3, 124.4, 123.7, 121.0, 112.9, 107.9, 106.2, 97.9, 69.7, 66.2, 65.9, 44.30, 12.6; IR (KBr, cm^{-1}): 3460, 3065, 1692; MS (FAB^+) m/z: calcd for $C_{74}H_{78}N_8O_7$: 1191.6; found: 1192.4 $(M+H)^+$; 1214.5 $(M+Na)^+$; Anal. calcd. for $C_{74}H_{78}N_8O_7$: C, 74.60; H, 6.60; N, 9.40; found C, 74.36; H, 6.97; N, 9.61.

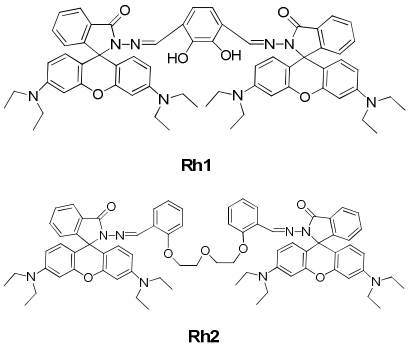

Fig. 1 Chemical structures of **Rh1** and **Rh2**.

Results and discussion

3.1 Colorimetric responses of sensor probes (Rh1 and Rh2) towards metal ions.

Selectivity is one of the most important characteristics in analyte–selective chemosensors. Initially, **Rh1**and **Rh2** (10 μM) in CH_3CN–H_2O (v/v = 9:1, 5mM Tris-HCl, pH 7.4) displayed no absorption bands corresponding to the rhodamine moiety. As shown in Figs. 2a and 2b, upon examine the selectivity of **Rh1** and **Rh2** towards various metal ions (4 equiv.), such as Li^+, Ag^+, K^+, Cs^+, Ni^{2+}, Fe^{3+}, Co^{2+}, Zn^{2+}, Cd^{2+}, Pb^{2+}, Ca^{2+}, Cr^{3+}, Cu^{2+}, Ba^{2+}, Al^{3+}, Fe^{2+}, Hg^{2+} and Mg^{2+}, the UV-vis spectra of **Rh1** and **Rh2** were only affected by Cu^{2+}, Fe^{3+} and Cr^{3+} ions to different extents. Among these three metal ions, upon the addition of Cu^{2+} both absorption bands of **Rh1** and **Rh2** had the largest changes with the absorption enhancements as large as 40 and 48 fold, respectively (Figs. S13a and S13b), where the detailed explanation will be discussed later. Sequentially, the maximum UV-vis absorption intensities of **Rh1** and **Rh2** at 561 nm were also increased upon the addition of Fe^{3+} (13 and 20 folds, respectively) or Cr^{3+} (8 and 10 folds, respectively) ions. Whereas, a significant increase in the absorption intensity at 561 nm may be attributed to the induced spirolactam ring opening upon the addition of metal ions. The photo images exhibit a naked eye colorimetric change of **Rh1** towards Cu^{2+} metal ion, where the most obvious and selective color change from colorless to pink color is observed in Fig. 3. Therefore, our careful investigations suggest that **Rh1** and **Rh2**could be useful as selective optical chemosensor towards Cu^{2+} than the other surveyed metal ions.

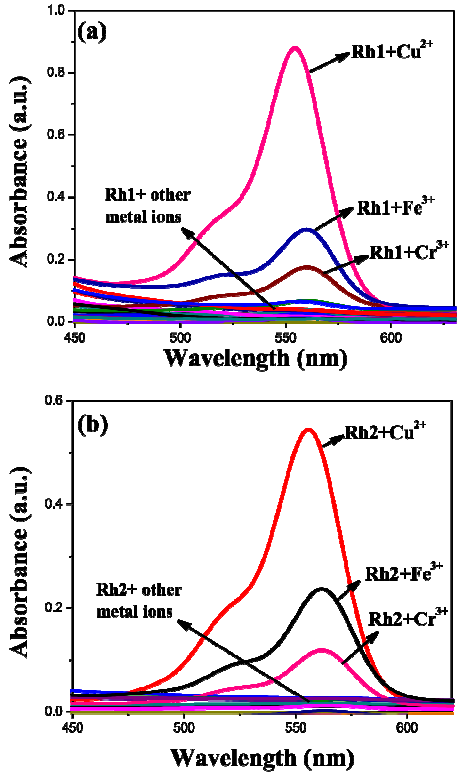

Fig. 2 UV-visible absorption spectra (a) **Rh1** and (b) **Rh2** (10μM) upon the addition of several relevant metal ions in CH_3CN–H_2O (v/v = 9:1, 5mM Tris-HCl, pH 7.4).

View Article Online
DOI: 10.1039/C6RA24472F

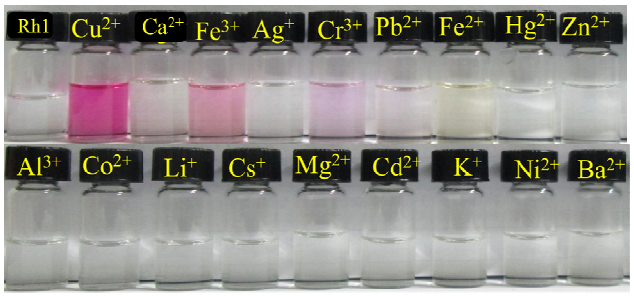

Fig. 3 Colorimetric changes (naked eye observations) of probe **Rh1** (1 μM) upon the addition of various metal ions (4 equiv.).

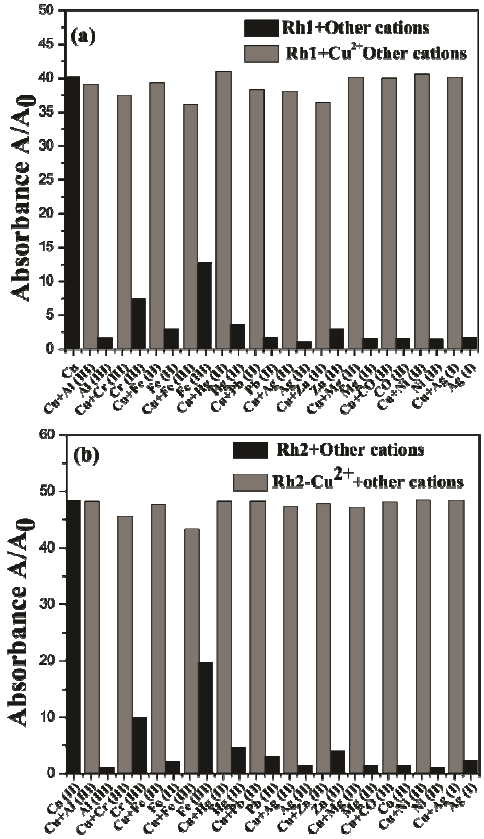

Fig. 4 (a) Absorbance changes of **Rh1** (10 μM) in CH_3CN–H_2O (v/v = 9:1, 5mM Tris-HCl, pH 7.4) solution upon the addition of 4 equiv. various metal ions (black bars). The grey bars represent the absorbance changes as 2.4 equiv. Cu^{2+} ion was added to the mixture of **Rh1** (10 μM) 4 equiv. Al^{3+}, Cr^{3+}, Fe^{3+}, Hg^{2+}, Pb^{2+}, Ag^{2+}, Zn^{2+}, Mg^{2+}, Ni^{2+} and Ag^{+} ions, respectively. (b) Absorbance changes of **Rh2** (10 μM) in CH_3CN–H_2O (v/v = 9:1, 5mM Tris-HCl, pH 7.4) solution upon the addition of 4 equiv. various metal ions (black bars). The grey bars represent the absorbance changes as 2.2 equiv. Cu^{2+} ion was added to the mixture of **Rh2** (10 μM) 4 equiv. Al^{3+}, Cr^{3+}, Fe^{3+}, Hg^{2+}, Pb^{2+}, Ag^{2+}, Zn^{2+}, Mg^{2+}, Ni^{2+} and Ag^{+} ions, respectively.

Furthermore, to explore the possible applications of **Rh1** and **Rh2** as practical cation-selective chromogenic chemosensors for Cu^{2+}, two competitive experiments were also carried out by monitoring the changes in UV-vis absorption intensities at 555 nm. To perform these dual metal ion experiments, **Rh1** and **Rh2** (10 μM) were first mixed with 4 equiv. of various metal ions including Al^{3+}, Cr^{3+}, Fe^{3+}, Hg^{2+}, Pb^{2+}, Ag^{2+}, Zn^{2+}, Mg^{2+}, Ni^{2+} and Ag^{+} ions, followed by the addition of 2 equiv. Cu^{2+} in CH_3CN–H_2O (v/v = 9:1, 5mM Tris-HCl, pH 7.4) solution. In the presence of miscellaneous competitive cations, the observations of UV-vis spectra for **Rh1** and **Rh2** did not show any changes in contrast to single Cu^{2+} ion experiments. However, in contrast to Cu^{2+} ion, only the cases of Fe^{3+} and Cr^{3+} ions were evidenced to affect the absorbtion peaks to some extents, as illustrated in Figs. 4a and 4b, where the significant spectral and color changes in dual metal ion systems with Cu^{2+} were still observed. Therefore, both designed dimeric probes (**Rh1** and **Rh2**) may be promising towards establishing selective colorimetric sensors for Cu^{2+} ion over the other competing metal ions.

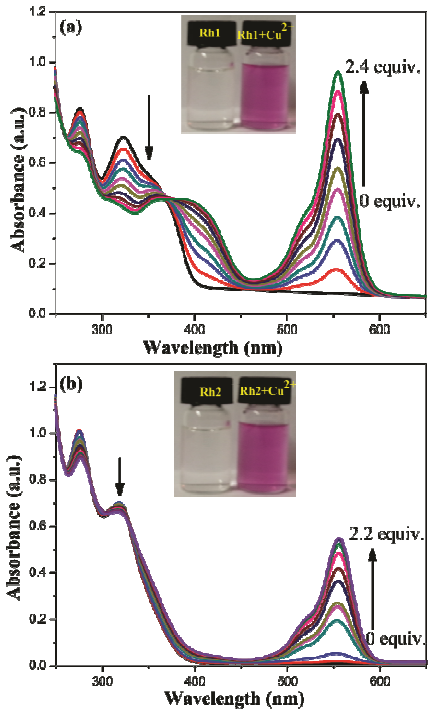

Fig. 5 The absorption spectral changes of (a) **Rh1** and (b) **Rh2** (10μM in CH_3CN–H_2O (v/v = 9:1, 5mM Tris-HCl, pH 7.4)) solution during the sequential additions of Cu^{2+}.

The spectroscopic properties of **Rh1** and **Rh2** (10μM) were investigated in a solvent system of in CH_3CN–H_2O (v/v = 9:1, 5mM Tris-HCl, pH 7.4). As shown in Fig. 5a, the free chemosensor **Rh1** exhibited an absorption band centered at 323 nm. Upon the addition of Cu^{2+} ion (0-2.4 equiv.) into **Rh1** solution, the absorption intensity at 323 nm gradually decreased with a simultaneous new absorption band appearance at 555 nm due to the possible formation of phenoxide ion, which can be further proven by later discussion. Interestingly, the absorption intensity as well as absorption position at isosbestic point 366 nm were remained constant during the interaction of Cu^{2+} with **Rh1** solution. Moreover, the absorbance values at 323 nm and 555 nm became saturated and leveled off with

View Article Online
DOI: 10.1039/C6RA24472F

2.4 equiv. of Cu^{2+} ion, and thus demonstrated the formation of a 1:2 complexations between the chemosensor **Rh1** and Cu^{2+} ion. The binding constant K_a and the calculated detection limit (LOD) were found to be 6.18 x 10^6 M^{-1} and 1.22 x 10^{-8} M (Figs. S14a and S15a), respectively.

Similarly, free **Rh2** Chemosensor was colorless as shown in Fig. 5b, when Cu^{2+} was added from 0 to 2 equiv., an absorption band at 556 nm gradually increased with respect to the concentrations of Cu^{2+} ion, which induced an optical color change from colorless to pink color. Therefore, a selective colorimetric change was observed only in the presence of Cu^{2+} ion, which was attributed to the spirolactum ring opening mechanism and multiple ether units reported in a previous literature.[54] The visible color change of **Rh2** towards Cu^{2+} clearly demonstrates that **Rh2** was highly sensitive to Cu^{2+}. Moreover, the binding affinity of **Rh2** towards Cu^{2+} was evaluated from UV-vis titration with an association constant K_a = 2.53x10^5 M^{-1} and its detection limit was estimated as 8.0x10^{-7} M (see Figs. S14b and S15b; ESI). Furthermore, after careful investigation of the fluorescence properties of dimeric systems **Rh1** and **Rh2**, we have established that they could not induce any fluorescence changes with all metal ions, including Cu^{2+} ion (see Figs. S16a and S16b; ESI). The fluorescence quenching process was accompanied by the inherent quenching property of paramagnetic Cu^{2+} ion. The proposed binding mechanism of dimeric sensor systems was monitored by the UV-vis absorption spectra. In the absence of Cu^{2+}, **Rh1** and **Rh2** displayed no absorbance above 400 nm, which indicated the closed spirolactum ring at this condition. Whereas, upon the addition of Cu^{2+} a new absorption band appeared at 555 nm suggested the disclosure of the spirolactum ring in the rhodamine unit. Therefore, we believe that the significant color change was solely due to the alteration of molecular structures between cyclic-spiro and ring-opening conformations of the rhodamine framework. Therefore, these observations suggested that among all metal ions only Cu^{2+} could induce the spirolactum ring opening of the rhodamine unit.

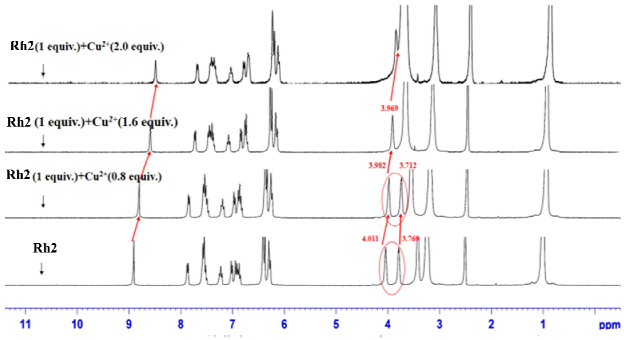

Fig. 6 ^{1}H NMR spectral changes of **Rh2** (10 mM) in DMSO-d_6 and titrated with 0-2.0 equiv. of Cu^{2+} in D_2O.

To further investigate the binding sites of dimeric systems, we did the ^{1}H NMR titrations of probes **Rh1** and **Rh2** in the presence of Cu^{2+} metal ion. To perform the experiments, **Rh1** and **Rh2** were dissolved in DMSO-d_6 (1 x 10^{-3} M) and Cu^{2+} solution (5 x 10^{-2} M) was prepared in D_2O. After adding Cu^{2+} (0-2 equiv.) sequentially into **Rh1** solution (1 equiv.), the total disappearance of -OH peak at 10.62 ppm (see Fig. S17), was well verified the clear binding of **Rh1** with Cu^{2+} ion through the phenoxide interactions (after the deprotonation of –OH due to binding with Cu^{2+}). In addition, owing to the Schiff-base binding of nitrogen atom with Cu^{2+} ion, the –CH proton peak was upfield-shifted from 9.07 to 8.59 ppm. In the case of **Rh2** (see Fig. 6), during the addition of Cu^{2+} (0-2 equiv.), the Ha (–CH_2) protons of the multiple ether unit (i.e., -O–CH_2–CH_2–O-) were upfield-shifted from 4.01 to 3.94 ppm. Similarly, the H_b (–CH_2) protons (with a lower polarity) at 3.77 ppm were also upfield-shifted in the above experiment. Further, the little upfiled-shifts of Schiff-base protons (i.e., -N=CH-) were observed because of the complex formation between 'N' atoms and Cu^{2+}. Hence, based on the ^{1}H NMR titrations, a possible mechanism is proposed in Scheme 1 to explain the binding mode of probes **Rh1** and **Rh2** towards Cu^{2+}.

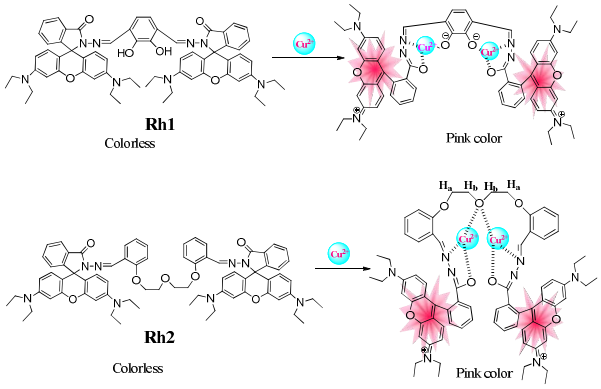

Scheme 1 A possible proposed binding mechanism of sensor probes **Rh1** and **Rh2** towards Cu^{2+}.

Additionally, to ensure the binding site of **Rh1** and **Rh2** towards Cu^{2+}, the stoichiometries of Cu^{2+} complexes (i.e., **Rh1**-Cu^{2+} and **Rh2**-Cu^{2+}) were determined from job's plots (see Figs. S18a and S18b; ESI) by fixing the final concentrations of **Rh1** -Cu^{2+} and **Rh2**-Cu^{2+} as 50μM. The stoichiometries of both metal complexes were established by job's plots between the mole fractions (Xm) and the maximum absorption changes at 553 nm and 556 nm for **Rh1**-Cu^{2+} and **Rh2**-Cu^{2+}, respectively. After attaining the maximum values, the absorption peaks at 553 and 556 nm were slowly reduced from 0.6 molar fraction of Cu^{2+}. Therefore, these phenomena clearly indicated the formation of 1:2 stoichiometric complexes for both dimeric systems towards Cu^{2+}. To reconfirm the Cu^{2+} binding mode of the dimeric systems (**Rh1** and **Rh2**), their FT-IR band (See Figs. S19a and S19b; ESI) of -OH at 3425 cm^{-1} and the ether linkage band (i.e., C-O-C) at 3460 cm^{-1} were investigated in the presence of Cu^{2+} ion. Correspondingly, the IR bands of C=O (at 1706 and 1692 cm^{-1}) and -C-H (at 3079 and 3065 cm^{-1}) were also been evaluated for **Rh1** and **Rh2** dimeric systems. During the complex formation of probes **Rh1** and **Rh2** to Cu^{2+} ion, the above characteristic bands were affected incredibly as noted next. The characteristic bands of -OH and ether unit are became very broad along with the disappearance of -CH bands of **Rh1** and **Rh2** at 3079 and 3065 cm^{-1}, respectively. Further to note, the respective C=O stretching bands of **Rh1** and **Rh2** at 1706 and 1692 cm^{-1} were also diminished with slight shift. The above FTIR changes were well confirmed the attachment of colorimetric probes **Rh1** and **Rh2** towards Cu^{2+} ion.

The reversibilities of sensor complexes **Rh1**-Cu^{2+} and **Rh2**-Cu^{2+} in in CH_3CN–H_2O (v/v = 9:1, 5mM Tris-HCl, pH 7.4) solutions are

View Article Online
DOI: 10.1039/C6RA24472F

important for future applications. The reversible nature of the sensor complexes with Cu^{2+} ion was further carried out through UV-vis observations by adding penta-methyl ethylene-triamine (PMDTA), which is a well-known metal ion chelator. As depicted in Figs. S20a and S20b (ESI), upon the addition of PMDTA (2.6 and 2.2 equiv.) to the mixtures of **Rh1**-Cu^{2+} and **Rh2**-Cu^{2+} (10 μM), the absorption bands were found to be restored immediately. Moreover, by increasing the concentration of PMDTA (0-2.6 equiv. and 0-2.2 equiv., respectively) the reversiblities of **Rh1**-Cu^{2+} and **Rh2**-Cu^{2+} with PMDTA were clearly established as shown in Figs. 21a and 21b (ESI). Upon the addition of PMDTA, the absorption peaks of dimeric probes **Rh1** and **Rh2** were decreased gradually to characterize the reversible sensing capabilities of sensor probes (**Rh1** and **Rh2**). This reversibility allow us to reuse of the sensor probes for effective Cu^{2+} detection.

3.2 Colorimetric responses of metal complexes (Rh1-Cu^{2+} and Rh2-Cu^{2+}) towards anions

Next, we used the previously formed metal complexes **Rh1**-Cu^{2+} and **Rh2**-Cu^{2+} to examine their anion selectivities. The absorbance spectral studies of metal complexes with different anions F^-, CN^-, HPO_4^{2-}, $H_2PO_4^-$, HSO_4^-, ClO_4^-, Br^-, OH^-, SCN^-, $P_2O_7^{4-}$, NO_3^- and OAc^- were carried out in the solution condition of 10μM in CH_3CN–H_2O (v/v = 9:1, 5mM Tris-HCl, pH 7.4). The color changes for metal complexes (**Rh1**-Cu^{2+} and **Rh2**-Cu^{2+}) towards various anions are demonstrated in the photograph images of Fig. 7, where no color changes were observed in all anions, except pyrophosphate (PPi).

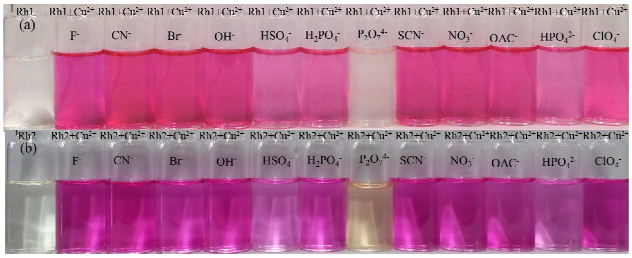

Fig. 7 Photo-images of color changes for metal complexes (**Rh1**-Cu^{2+} and **Rh2**-Cu^{2+}) towards various anions.

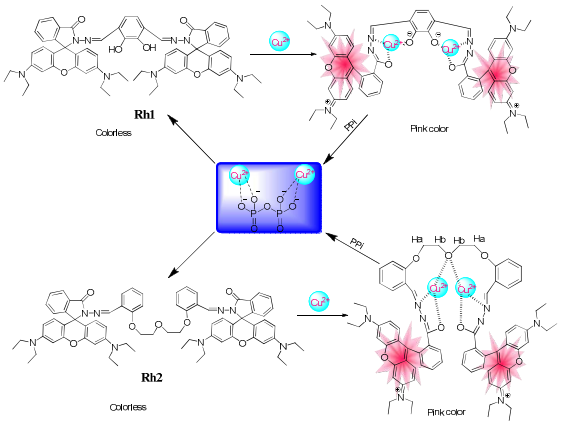

Scheme 2 Possible proposed sensing mechanism of metal complexes (**Rh1**-Cu^{2+} and **Rh2**-Cu^{2+}) towards pyrophosphate (PPi) anion.

The addition of PPi anion turned the original pink colored solution into a colorless solution. Upon the addition of PPi (1 equiv.), not only these color changes could be easily recognized by naked-eyes, but also the UV-vis spectral changes were apparent as noticed in Figs. 8a and 8b. On the other hand, metal complexes didn't show any considerable spectral changes in absorption peaks during the addition of other anions (up to 4 equiv.). Therefore, the selectivity of the metal complexes (**Rh1**-Cu^{2+} and **Rh2**-Cu^{2+}) towards PPi anion might be attributed to their release of **Rh1** and **Rh2** through the strong binding affinity of PPi to copper ion as illustrated in Scheme 2. This result indicates that both metal complexes can serve as potential candidates as "naked-eye" chemosensor for PPi detection in semi-aqueous medium. Meanwhile, we further investigated the binding properties of both metal complexes by UV-vis titration experiments. Fig. 9 showed the colorimetric changes of metal complexes (**Rh1**-Cu^{2+} and **Rh2**-Cu^{2+}) 10 μM in in CH_3CN–H_2O (v/v = 9:1, 5mM Tris-HCl, pH 7.4). Upon the addition of increasing concentrations (1 equiv.) of PPi, the absorbance at 554 nm was decreased linearly with increasing the concentration of PPi.The binding constants between the metal complexes (**Rh1**-Cu^{2+} and **Rh2**-Cu^{2+}) and PPi were calaulcated as 1.09 x $10^5 M^{-1}$ and 4.11 x10^4 M^{-1}, respectively (see Figs. S22a and S22b; ESI). Furthermore, based on the results of UV-vis titrations, the detection limits of metal complexes (**Rh1**-Cu^{2+} and **Rh2**-Cu^{2+}) mediated PPi sensors were estimated to be 0.389 x 10^{-6} M and 1.61 x 10^{-6} M, respectively, as shown in Figs. S23a and 23b (ESI). These observations suggest that both metal complexes (**Rh1**-Cu^{2+} and **Rh2**-Cu^{2+}) could be excellent chemosensors for the detection of PPi anion.

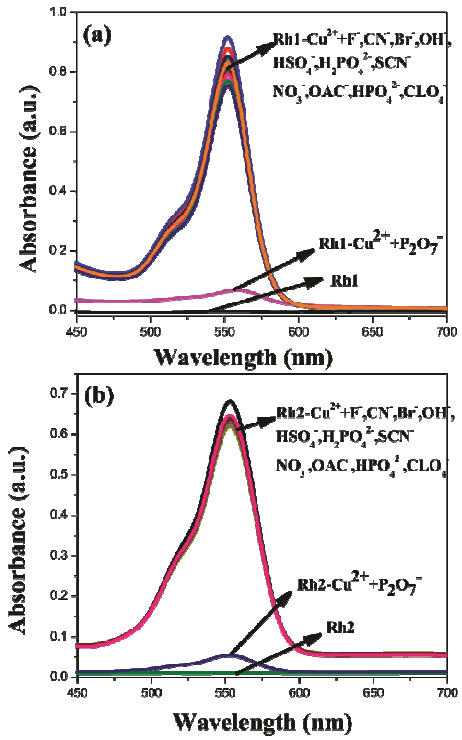

Fig 8. (a) UV-visible spectral changes of **Rh1**-Cu^{2+} and (b) **Rh2**-Cu^{2+} (10 μM) upon the addition of several relevant anions in CH_3CN–H_2O (v/v = 9:1, 5mM Tris-HCl, pH 7.4).

View Article Online
DOI: 10.1039/C6RA24472F

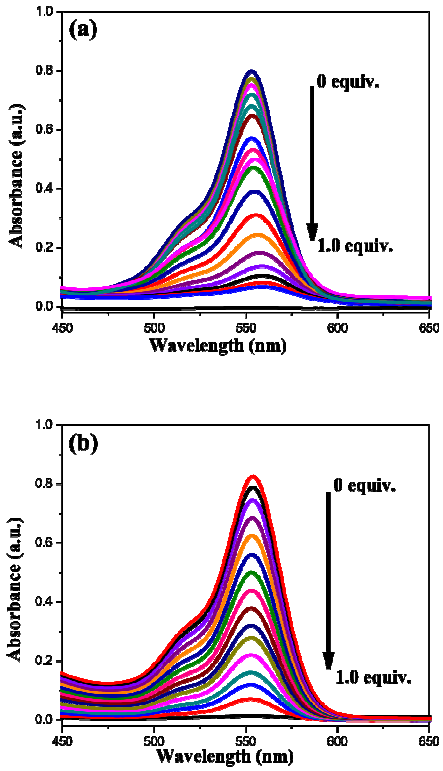

Fig. 9 Absorption spectral changes of (a) **Rh1**-Cu^{2+} and (b) **Rh2**-Cu^{2+} (10μM) in CH_3CN–H_2O (v/v = 9:1, 5mM Tris-HCl, pH 7.4) during the sequential additions of PPi.

For practical applications, we need to evaluate the utilizations of colorimetric sensor probes under wider pH conditions (other than the previous neutral form). As expected, the absorption peaks of un-bonded **Rh1** and **Rh2** (without Cu^{2+}) were only observable in the ranges of pH=2.0-5.0, suggesting that the strong protonation and spirolactum ring opening process of sensor probes occurred at certain pH ranges. In order to investigate the applications of **Rh1** and **Rh2** over a wide pH span of 0-12, the absorption intensities of **Rh1** and **Rh2** increased by adding Cu^{2+} under pH=3.0-8.0 (see Figs. S24a and S24b; ESI). In this pH zone, Cu^{2+} induced unique ring opening process in the rhodamine unit was obtained, which clearly demonstrated **Rh1** and **Rh2** as effective colorimetric probes towards Cu^{2+} under environmental conditions.

3.3 Theoretical calculations

To evaluate the experimental observations and provide a better insight into probes **Rh1** and **Rh2** along with their Copper complexes, the DFT and TD-DFT calculations were carried out and summarized in Table 1. The model structures have been built for **Rh1** and its copper complex as shown in Fig. 10.

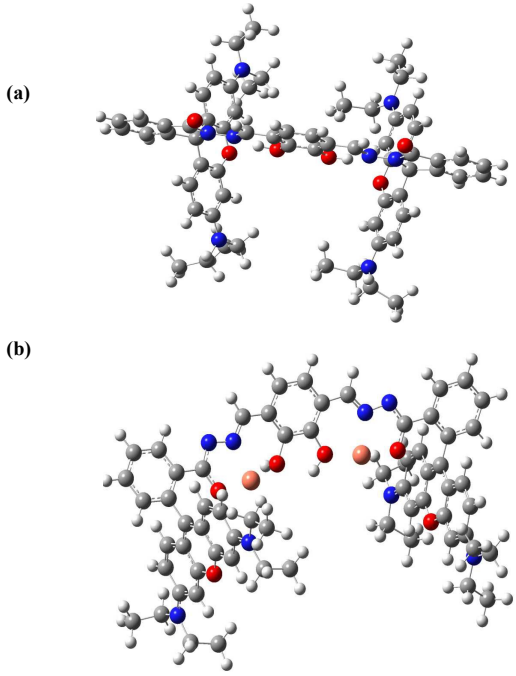

Fig. 10 Optimized structures of (a) **Rh1** and (b) complex **Rh2**-Cu^{2+} at B3LYP/LANL2DZ in the gas phase.

The main absorption bands of transitions were H-->L, H-->L+2, H-->L+1 and H-->L+1 observed in **Rh1**, **Rh1**-Cu^{2+}, **Rh2** and **Rh2**-Cu^{2+}, respectively. Fig. 11 shows the molecular orbital of **Rh1**, where the electron density of HOMO was located partially on the catechol unit and further on the oxa-anthracene unit and the LUMO was partially located on the catechol unit and further at the indole units on both sides. As shown in Fig. 12, the electron density of HOMO in complex **Rh1**-Cu^{2+} was located on the hydrazine units with part of **Rh2**-Cu^{2+} are shown in Figs. S25a and S25b (ESI). The respective molecular orbitals of **Rh2** and **Rh2**-Cu^{2+} are shown in Figs. S26 and S27 (ESI). As shown in Fig. S26 (ESI) in **Rh2**, the electron density of HOMO was located on a spiro unit, and that of LUMO was also located on a spiro unit. The electron density of HOMO has been shifted slightly towards the edge of the spiro unit in **Rh2**-Cu^{2+} complex. The LUMO also covered partially one Cu^{2+} unit with aza-carbonyl and benzene units of the complex. From the molecular orbitals of probes and complexes (Figs. 10, 11, S26 and S27), the electron densities located on the same part of the HOMO and LUMO for the cases of **Rh2** and **Rh2**-Cu^{2+}, but on the different parts of HOMO and LUMO for the cases of **Rh1** and **Rh1**-Cu^{2+}. Based on our calculated molecular orbital diagram in Fig. 11, the conjugated system was broken due to the addition of Cu^{2+} which led to the stronger ICT mechanism[55-56] in the Cu^{2+} complexes. This could be the possible explanations for the experimental observations of ratiometric responses of the Cu^{2+} complexes. Furthermore, the HLG value was also reduced in complex **Rh1**-Cu^{2+} (2.10 eV) in contrast to that of **Rh1** (2.64 eV).

View Article Online
DOI: 10.1039/C6RA24472F

Journal Name

ARTICLE

Table 1 The predicted values of HOMO, LUMO, HOMO LUMO gap (HLG) and oscillator strength (f) for **Rh1**, **Rh1**+Cu^{2+}, **Rh2** and **Rh2**+Cu^{2+} by DFT and TD-DFT calculations

System	Tot.E[a]	HOMO (eV)	LUMO (eV)	HLG (eV)[b]	Excited States	f[c]	Contribution
Rh1	-3367.381623	-4.269328	-1.625269	2.64	S1	0.0475	H-->L (0.69) H-->L+1 (-0.1)
					S2	0.0146	H-1 --> L (0.69) H-1 --> L+1 (0.1)
Rh1+Cu^{2+}	-3759.353208	-7.281195	-5.181813	2.10	S1	0.0001	H-->L+2 (0.6) H-->L+3 (-0.33) H-->L+5 (0.16)
					S2	0.0477	H-->L+2 (0.34) H-->L+3 (0.61)
Rh2	-3830.768067	-4.172246	-1.302659	2.87	S1	0.011	H-->L+1 (0.71)
					S2	0.009	H+1-->L+2 (0.7)
Rh2+Cu^{2+}	-4223.285313	-4.172246	-8.467632	1.28	S1	0.0025	H-->L+1 (0.7)
					S2	0	H+1--->L+1 (0.7)
					S3	0.0026	H+1--->L+2 (0.7)

[a] Total energy; [b] HOMO-LUMO gap; [c] oscillator strength.

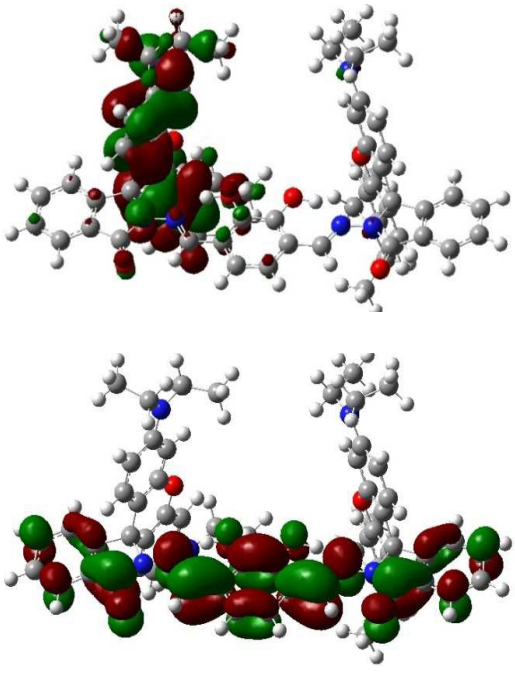

Fig. 11 HOMO-LUMO structures of **Rh1** at B3LYP/LANL2DZ level in the gas phase.

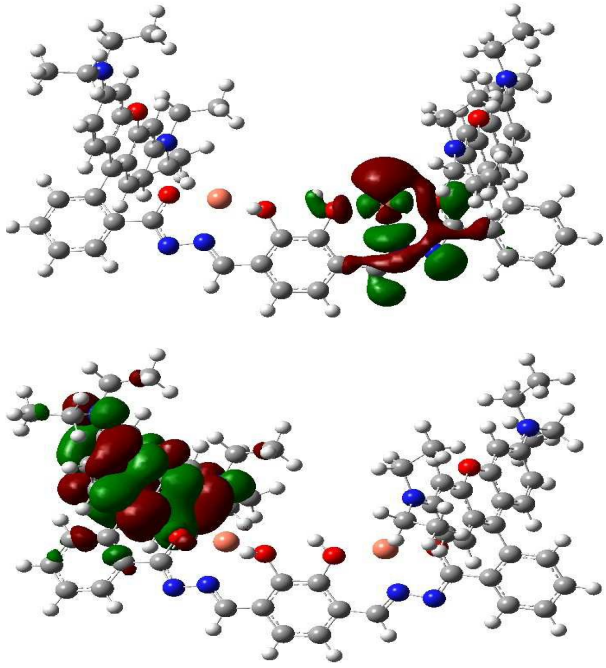

Fig. 12 HOMO-LUMO structures of complex **Rh1**+Cu^{2+} at B3LYP/LANL2DZ level in the gas phase.

View Article Online
DOI: 10.1039/C6RA24472F

3.4 Colorimetric responses on a solid support

In analytical chemistry grade, the sensitivity of a sensing system is crucial. Normally, it remains big challenges to achieve high sensitivities in such colorimetric sensing systems. We systematically investigated the selectivities, sensitivities and reversibilities of **Rh1** and **Rh2** on TLC plates coated with ready-made silica. Test strips were prepared by immersing silica gel plates into a CH_3CN solution of **Rh1** (10^{-4} M) and then were dried by a drier. As shown in Fig. 13, the strips were examined with various metal ions (10^{-3} M) by dipping into the corresponding solutions. We found that only copper ion induced a remarkable color change from colorless to pink, implying that probe was a highly selective naked-eye sensor probe towards Cu^{2+} over the other metal ions.

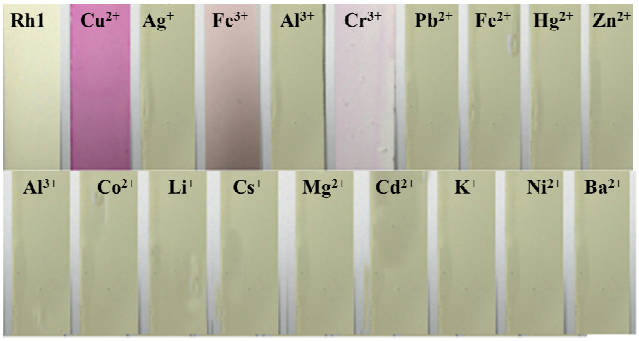

Fig. 13 Photographs of sensor tests on **Rh1** strips in the presence of various metal ions.

The detection results of test strips containing **Rh1** towards Cu^{2+} with different concentrations are also illustrated in Fig. S28. The higher concentration of copper ion, the more apparent color change from colorless to pink, where the detectable concentration of copper ion could be as low as 4 x 10^{-6} M. As shown in Fig. 14, further reversibility investigation revealed that the pink color of the test strips containing complex **Rh1**-Cu^{2+} faded out in the presence of PMDTA (10^{-5} M). Therefore, we have developed the notable and reversible naked-eye sensor strips to detect low concentrations of copper ion (4 μM) in this study. Similar results regarding selectivity, sensitivity and reversibility of test strips for **Rh2**were also been obtained (see Figs. S29-S31; ESI). Therefore, test strips containing **Rh1** and **Rh2** can conveniently detect aqueous copper ion, which demonstrate a cost-effective detection method without using any equipments.

4. Conclusions

We have developed reversible colorimetric probes **Rh1** and **Rh2** for the selective and sensitive sequential detections of Cu^{2+} and pyrophosphate *via* the ratiometric absorption spectral changes. Stoichiometry and binding mechanisms for both probes were well characterized and established by the respective spectroscopic techniques and theoretical calculations. Observations revealed a better performance of **Rh1** towards the selective and effective colorimetric detection of Cu^{2+} ion at a lower concentration than

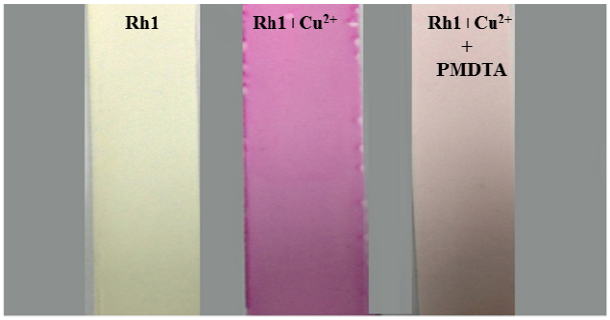

Fig. 14 Photographs of reversibility tests on **Rh1** strips (10^{-4} M) in the presence of **PMDTA** (10^{-5} M). From left to right: **Rh1**, **Rh1**-Cu^{2+} and **Rh1**-Cu^{2+}+**PMDTA**.

that of **Rh2**. Reversibility may open the avenue towards cost effectiveness and understanding the role of metal ions byswitching signals between structural transformations and thus for easy detections of analytes for societal demands. Detections of Cu^{2+} by the designed probes were performed in solution and on solid supports by simple titration and dipping of metal ion solutions (without utilizing any drastic conditions), which may push the limits of our designed probes to future concerning ecological problems as well as living systems. Importantly, **Rh1** and **Rh2** are good example of reversible rhodamine-based colorimetric probes for sequential detections of Cu^{2+} ion and PPi *via* ratiometric responses.

Acknowledgments

The financial supports of this project are provided by the Ministry of Science and Technology (MOST) in Taiwan through MOST 103-2113-M-009-018-MY3 and MOST 103-2221-E-009-215-MY3. Mr. parthiban venkatesan is acknowledged for his timely help during the paper writing.

References

1. Y. Yang, Q. Zhao, W. Feng and F. Li, *Chem. Rev*., 2012, **113**, 192-270.
2. Z. Liu, C. Peng, Z. Lu, X. Yang, M. Pei and G. Zhang, *Dyes Pigments,* 2015 **123**, 85-91.
3. X. Li, M. Yu, F. Yang, X. Liu, L. Wei and Z. Li, *New J. Chem.,* 2013, **37**, 2257-2260.
4. M. Shellaiah, Y. H. Wu, A. Singh, M.V. Ramakrishnam Raju and H.-C. Lin, *J. Mater. Chem. A,* 2013, **1**, 1310-1318.
5. D. Udhayakumari, S. Velmathi, W. C. Chen and S. P. Wu, *Sens. Actuators B.,* 2014, **204**, 375-381.
6. H. T. Feng S. Song Y. C. Chen C. H. Shen and Y. S. Zheng, *J. Mater. Chem. C.,* 2014, **2** ,2353-2359.
7. G. Sivaraman, T. Anand and D. Chellappa, *RSC Adv.*, 2013, **3**, 17029-17033.
8. Y. Zhou, F. Wang, Y. Kim, S. J. Kim and J. Yoon, *Org. Lett.*, 2009, **11**, 4442 – 4445.
9. P. Zhang, L. Pei, Y. Chen, W. Xu, Q. Lin, J. J. Wang, Wu, Y. Shen, L. Ji and H. Chao, *Chem.-Eur. J*., 2013, **19**, 15494-15503.
10. J. Jeong, B. A. Rao and Y. A. Son, *Sens. Actuators B*., 2015, **220**, 1254-1265.

View Article Online
DOI: 10.1039/C6RA24472F

11. E. Gaggelli, H. Kozlowski, D. Valensin and G. Valensin, *Chem. Rev.* 2006, **106**, 1995-2044.
12. M. Yang, W. Meng, X. Liu, N. Su, J. Zhou and B. Yang, *RSC Adv.,* 2014, **4**, 22288-22293.
13. G. Y. Lan, C. C. Huang and H. T. Chang, *Chem. Commun.*, 2010, **46**, 1257-1259.
14. Y. Chen, Y. Mi, Q. Xie, J. Xiang, H. Fan, X. Luo and S. Xia, *Anal. Methods,* 2013, **5**, 4818-4823.
15. H. S. Jung, P. S. Kwon, J. W. Lee, J. I. Kim, C. S. Hong, J. W. Kim, S. Yan, J. Y. Lee, J. H. Lee, T. Joo and J. S. Kim, *J. Am. Chem. Soc.,* 2009, **131**, 2008-2012.
16. M. Li, H. Ge, R.L. Arrowsmith, V. Mirabello, S. W. Botchway, W. Zhu, S. I. Pascu and T. D. James, *Chem. Commun*., 2014, **50**, 11806-11809.
17. D. Udhayakumari, S. Velmathi, Y. M. Sung and S. P. Wu, *Sens. Actuators B*., 2014, **198**, 285-293.
18. S. D. S. Parveen, B. S. Kumar, S. R. Kumar, R. I. Khan and K. Pitchumani, *Sens. Actuators B*., 2015, **221**, 75-80.
19. V. Tharmaraj and K. Pitchumani, *J. Mater. Chem. B*., 2013, **1**, 1962-1967.
20. D. Maity, A.K. Manna, D. Karthigeyan, T.K. Kundu, S.K. Pati and T. Govindaraju, *Chem.-Eur. J*., 2011, **17**, 11152-11161.
21. H. Kim, B. A. Rao, J. W. Jeong, S. Mallick, S. M. Kang, C. S. Choi, Y. A. Lee and Y. A. Son, *Sens Actuators B*., 2015, **210**, 173-182.
22. (a) N. Aksuner, E. Henden, I. Yilmaz and A. Cukurovali, *Dyes Pigments,* 2009, **83**, 211-217.(b) K. Ghosh, D. Tarafdar, A. Majumdar, C. G. Daniliuc, A. Samadder and A. R. Khuda-Bukhsh, *RSC Adv.,* 2016, **6**, 47802-47812. (c) G. Li, F. Tao, H. Wang, L. Wang, J. Zhang, P. Ge, L. Liu, Y. Tong and S. Sun, *RSC Adv.,* 2015, **5**, 18983-18989.(d) A. Rai, N. Kumari, R. Nair, K. Singh and L. Mishra, *RSC Adv.,* 2015, 5, 14382-14388.
23. Z. Li, W. Zhang, X. Liu, C. Liu, M. Yu and L. Wei, *RSC Adv.*, 2015, **5**, 25229-25235.
24. D. H Lee, S. Y. Kim and J. I. Hong, *Angew. Chem. Int. Ed*., 2004, **43**, 4777-4780.
25. J. H. Wang, J. B. Xiong, X. Zhang, S. Song, Z. H. Zhu and Y. S. Zheng, *RSC Adv.*, 2015, **5** , 60096-60100.
26. E. Quinlan, S. E. Matthews and T. Gunnlaugsson, *J. Org. Chem.,* 2007, **72**, 7497-7503.
27. (a) S. Bhowmik, B. N. Ghosh, V. Marjomäki and K. Rissanen, *J. Am. Chem. Soc.* 2014, **136**, 5543-5546.(b) S. Goswami, S. Paul and A. Manna, *RSC Adv.,* 2013, **3**, 10639-10643.
28. (a) P. Anzenbacher, M. A. Palacios, K. Jursíková and M. Marquez, *Org. Lett.,* 2005, **7**, 5027-5030.(b) S. Lee, K. K. Y. Yuen, K. A. Jolliffe and J. Yoon, *Chem. Soc. Rev.,* 2015, **44**, 1749-1762. (c) V. E. Zwicker, B. M. Long and K. A. Jolliffe, *Org. Biomol. Chem*., 2015, **13**, 7822-7829.
29. L. S. A. Haque, R. L. Bolhofner, B. M. Wong and M. A. Hossain, *RSC Adv.*, 2015, **5**, 38733-38741.
30. S. Kim, M. S. Eom, S. Yoo and M. S. Han, *Tetrahedron. Lett*., 2015, **56**, 5030-5033.
31. G. Sivaraman and D. Chellappa, *J. Mater. Chem. B.,* 2013, **1**, 5768-5772.
32. J. W. Jeong, B. A. Rao and Y. A. Son, *Sens. Actuators B.,* 2015, **208**, 75-84.
33. H. N. Kim, M. H. Lee, H. J. Kim, J. S. Kim and J. Yoon, *Chem. Soc. Rev*., 2008, **37**, 1465-1472.
34. Y. Q. Sun, J. Liu, X. Lv, Y. Liu, Y. Zhao and W. Guo, *Angew. Chem. Int. Ed*., 2012, **51**, 7634-7636.
35. L. Huang, X. Wang, G. Xie, P. Xi, Z. Li, M. Xu, Y. Wu, D. Bai and Z. Zeng, *Dalton. Trans.,* 2010, **39**, 7894-7896.
36. A. Chatterjee, M. Santra, N. Won, S. Kim, J. K. Kim, S. B. Kim and K. H. Ahn, *J. Am. Chem. Soc*., 2009, **131**, 2040-2041.
37. Z. Q. Hu, X. M. Wang, Y. C. Feng, L. Ding and H. Y. Lu, *Dyes Pigments.,* 2011, **88**, 257-261.
38. F.-M. Yang, W. Meng, Q. Ding, N. Su, X. Liu, M. Zhang B and Yang, *New J. Chem.*, 2015, **39**, 4790-4795.
39. S. D. S. Parveen, A. Affrose and K. Pitchumani, *Sens. Actuators B* 2015, **221**, 521-527.
40. B. Imene, Z. Cui, X. Zhang, B. Gan, Y. Yin, Y. Tian, H. Deng and H. Li, *Sens. Actuators, B*., 2014, **199**, 161-167.
41. S. Jayabal, R. Sathiyamurthi and R. Ramaraj, *J. Mater. Chem. A.,* 2014, **2**, 8918-8925.
42. Q. Li, Y. Guo, J. Xu and S. Shao, *Sens. Actuators B* 2011, **15**, 427-431.
43. H. Li, Z. Cui and C. Han, *Sens. Actuators, B*. 2009, **143**, 87-92.
44. J. Y. Noh, G. J. Park, Y. J. Na, H. Y. Jo, S. A. Lee and C. Kim, *Dalton Trans.,* 2014, **43**, 5652-5656.
45. Y. Lv, Y. Guo, J. Xu. and S. Shao, *Fluorine Chem*., 2011, **132**, 973-977.
46. G. Sivaraman, T. Anand and D. Chellappa, *Analyst*, 2012, **137**, 5881-5884.
47. M. J. Culzoni, A. Munoz de la Pena, A. Machuca, H. C. Goicoechea and R. Babiano, *Anal. Methods,* 2013, **5**, 30-49.
48. C. R. Lohani, J. M. Kim, S. Y. Chung, J. Yoon and K. H. Lee. *Analyst.,* 2010, **135**, 2079-2084.
49. M. J. Frisch, G. W. Trucks, H. B. Schlegel, G. E. Scuseria, M. A. Robb, J. R. Cheeseman, G. Scalmani, V. Barone, B. Mennucci, G. A. Petersson, H. Nakatsuji, M. Caricato, X. Li, H. P. Hratchian, A. F. Izmaylov, J. Bloino, G. Zheng, J. L. Sonnenberg, M. Hada, M. Ehara, K. Toyota, R. Fukuda, J. Hasegawa, M. Ishida, T. Nakajima, Y. Honda, O. Kitao, H. Nakai, T. Vreven, J. A. Montgomery, Jr. J. E. Peralta, F. Ogliaro, M. Bearpark, J. J. Heyd, E. Brothers, K. N. Kudin, V. N. Staroverov, R. Kobayashi, J. Normand, K. Raghavachari, A. Rendell, J. C. Burant, S. S. Iyengar, J. Tomasi, M. Cossi, N. Rega, J. M Millam, M. Klene, J. E. Knox, J. B. Cross, V. Bakken, C. Adamo, J. Jaramillo, R. Gomperts, R. E. Stratmann, O. Yazyev, A. J. Austin, R. Cammi, C. Pomelli, J. W. Ochterski, R. L. Martin, K. Morokuma, V. G. Zakrzewski, G. A. Voth, P. Salvador, J. J. Dannenberg, S. Dapprich, A. D. Daniels, Ö. Farkas, J. B. Foresman, J. V. Ortiz, J. Cioslowski, D. J. Fox, *Gaussian Inc Wallingford* CT 2009.
50. A. D. Becke, *J. Chem. Phys.,* 1997, **107**, 8554-8560.
51. P. Gou, N. D. Kraut, I. M. Feigel and A. Star, *Macromolecules*., 2013, **46**, 1376-1383.
52. K. D. Belfield, M. V. Bondar, A. Frazer, A. R. Morales, O. D. Kachkovsky, I. A. Mikhailov, A. M. E. Masunov and O. V. Przhonska, *J. Phys. Chem. B*, 2010, **114**, 9313-9321.
53. X. Zhang and Y. Y. Zhu, *Sens. Actuators, B.* 2014, **202**, 609-614.
54. H. Y. Lee, K. M. K. Swamy, J. Y. Jung, G. Kim and J. Yoon, *Sens. Actuators B.,* 2013, **182**, 530-537.
55. H. S. Jung, K. C. Ko, G. H. Kim, A. R. Lee, Y. C. Na, C. Kang, J. Y. Lee and J. S. Kim, *Org. Lett.*, 2011, **13**, 1498-1501.
56. L. Deng, W. Wu, H. Guo, J. Zhao, S. Ji, X. Zhang, X. Yuan and C. Zhang, *J. Org. Chem.*, 2011, **76**, 9294-9304.

View Article Online
DOI: 10.1039/C6RA24472F

Table of Contents (TOC)/ABSTRACT Graphic

Two rhodamine hydrazine derivatives **Rh1** and **Rh2** with catechol and ether functionalities have been synthesized and utilized towards sequential colorimetric detections of Cu(II) and pyrophosphate (PPi) ions in $CH_3CN–H_2O$ (v/v = 9:1, 5mM Tris-HCl, pH 7.4) semi-aqueous medium.